HHS Public Access

Author manuscript

J Biomed Mater Res A. Author manuscript; available in PMC 2015 May 17.

Published in final edited form as:

J Biomed Mater Res A. 2013 August ; 101(8): 2313–2321. doi:10.1002/jbm.a.34543.

Dynamic and reversible surface topography influences cell morphology

Jennifer D. Kiang[1], **Jessica H. Wen**[1], **Juan C. del Álamo**[2], and **Adam J. Engler**[1,3]

[1]Department of Bioengineering, University of California, San Diego, La Jolla, California 92093

[2]Department of Mechanical and Aerospace Engineering, University of California, San Diego, La Jolla, California 92093

[3]Sanford Consortium for Regenerative Medicine, La Jolla, California 92037

Abstract

Microscale and nanoscale surface topography changes can influence cell functions, including morphology. Although *in vitro* responses to static topography are novel, cells *in vivo* constantly remodel topography. To better understand how cells respond to changes in topography over time, we developed a soft polyacrylamide hydrogel with magnetic nickel microwires randomly oriented in the surface of the material. Varying the magnetic field around the microwires reversibly induced their alignment with the direction of the field, causing the smooth hydrogel surface to develop small wrinkles; changes in surface roughness, ΔR_{RMS}, ranged from 0.05 to 0.70 μm and could be oscillated without hydrogel creep. Vascular smooth muscle cell morphology was assessed when exposed to acute and dynamic topography changes. Area and shape changes occurred when an acute topographical change was imposed for substrates exceeding roughness of 0.2 μm, but longer-term oscillating topography did not produce significant changes in morphology irrespective of wire stiffness. These data imply that cells may be able to use topography changes to transmit signals as they respond immediately to changes in roughness.

Keywords

roughness; microwire; magnetic field; polyacrylamide; cell area

INTRODUCTION

Extracellular matrix, the material that surrounds cells and facilitates their attachment, has tissue specific composition, elasticity, and topography that changes with time as cells remodel and pull on it to mediate cell communication.[1,2] Vascular smooth muscle cells (VSMCs) are highly sensitive to such physical matrix cues, most notably matrix elasticity.[3,4] However despite VSMCs living in a dense, fibrillar matrix, we know comparatively little

Correspondence to: A. J. Engler; aengler@ucsd.edu.

Additional Supporting Information may be found in the online version of this article.

about how VSMCs respond to topographical cues, let alone their response to dynamic changes in topography.

Several different substrate types have been fabricated to better understand how topography influences cell behavior in an attempt to answer this question. Grooves, pillars/ wells, and islands/pits have been etched or cut into rigid substrates,[5–7] and in most cases, stem cell osteogenesis was observed with the degree of induction depending on feature geometry, feature size,[6,8] and spatial organization.[9] Although responses to static surfaces are intriguing, VSMCs are constantly reorganizing matrix and topography *in vivo*, and thus a more biomimetic material should accommodate remodeling on-demand. Compression of an oxidized layer of polydimethylsiloxane has been used to make a substrate that creates reversible, grooved features[10], but given a relatively low curing ratio, these substrates were likely seen as rigid relative to VSMCs' normally soft niche.[11,12] Softer materials, including electrospun fibers, nicely illustrate how VSMCs can respond and remodel the fiber network,[13] but the remodeling is difficult to control and typically irreversible.[14] Shape memory polymers have also been used to alter topography, are soft, and can be reversible.[15,16] However, these systems rely on materials and transition temperatures—often well below 37°C—that may not be ideally suited for cell culture, and their transition times, ~hours,[15] are longer than typical cell-matrix remodeling, which takes place in ~minutes.[1]

Understanding cell responses to controlled, dynamic changes in topography could help us better understand how *in vivo* topography-driven changes from matrix overexpression during atherosclerosis[17] affect cytoskeletal assembly. Static topography features of varying size and organization can all be fabricated with rigid structures, that is, polydimethylsiloxane, poly(methylmethacrylate), polystyrene, silicon, and carbon nanotubes,[5–9] but controllable, dynamic features are easier to create in compliant substrates, which have an inherent Young's modulus, *E*, or "stiffness" (measured in Pascals, Pa) that is substantially lower than the rigid materials used in making static features. Substrate stiffness has been previously documented to influence MSC differentiation, [18–20] and so topography effects thus far may be complicated by the use of rigid materials. Here, we have redesigned the classically used polyacrylamide (PA) hydrogel system to create a new cell culture substrate that, when magnetically actuated, can reversibly induce random surface topographies in a soft material to which cells can respond.

MATERIALS AND METHODS

Microwire fabrication

To fabricate microwires, a 50 cm segment of 0.025-mm diameter nickel wire (#40672, Alfa Aesar) was used, cut it into ~1 cm lengths, and etched in a dilute acid solution of one part nitric acid and one part dH_2O (prepared immediately before use) for 20 min to produce a wire diameter of ~5 μm. Diluting the acid solution with water terminated the etching process. Wires were embedded and aligned by a magnetic field in optimal cutting temperature (OCT) compound. Once the wires were frozen in solid state OCT, they were cut perpendicular to their long axis using a cryostat (Leica CM 1950), creating 20 μm long microwires. To purify the wires, OCT sections were diluted with 10 mL of dH_2O, mixed, and centrifuged for 5 min at 2000 RPM to sediment the OCT and any remaining debris. The

wires were then precipitated with a magnet, and the remaining solution discarded. Wires were resuspended in dH_2O, mixed, and spun again. Wires were precipitated again and the solution decanted. Wires were finally suspended in dH_2O, vortexed for 30 s, sonicated for 10 min, autoclaved, and vortexed and sonicated again immediately prior to every use.

Microwire-embedded hydrogel synthesis

Amino-activated glass coverslips were made based on previous methods.[21] Briefly, aminosilanation was achieved by drying NaOH uniformly onto the coverslip, adding APES, washing with dH_2O, and incubating in gluteraldehyde. 20 μL of a 5% acrylamide and 0.03% bis-acrylamide polymer solution, which normally produces a hydrogel with $E \sim 1$ kPa,[21] were placed on hydrophobic dichlorodimethylsiloxane-coated slides to ensure that the hydrogels would only adhere to the amino-activated coverslips, which were subsequently added on top of the polymer solution prior to polymerization with ammonium persulfate and tetramethylethy-lenediamine. Once the first hydrogel layer was polymerized, the aminosilanated coverslip with attached hydrogel was separated from the slide, and a 20 μL drop of wire solution was added on top of the hydrogel and carefully spread with the side of a 20 μL pipette tip. Residual water sitting on the hydrogel was removed, and 8 μL of a second polymer solution of identical composition but also containing 0.1 μm fluorescent microspheres was added to the first hydrogel layer. For our purposes, the only relevant deformation was in the surface of the hydrogel, thus fluorescent beads were only added to the top hydrogel layer. The system was again inverted and placed onto a dichlorodimethylsiloxane-coated slide. Once the second layer had polymerized, the hydrogel was rinsed in dH_2O and allowed to swell for at least 30 min. To promote cell adhesion, the coverslip was immersed in Sulfo-SANPAH, a heterobifunctional protein cross-linker, and activated by 305 nm UV light for 10 min. The hydrogel was then washed three times in HEPES buffer under sterile conditions and incubated with 10 μg/mL of human fibronectin at 37°C for at least 2 h, a process which has been shown to enable sufficient cell adhesion.[22] The hydrogels were then kept in PBS until use. Fibronectin was visualized using a polyclonal primary antibody, R457,[23] and FITC-labeled goat anti-rabbit secondary antibody. Confocal imaging was performed as described below.

Material characterization-topography

Wires were aligned with two NdFeB block magnets, each exerting a magnetic field of 0.31 T,[24] to create a field perpendicular to the functionalized surface of the hydrogel. The topographical changes induced by this field were measured using traction force microscopy image analysis software[25] where the three-dimensional movement of fluorescent beads as a result of the magnetic field was tracked. Two sets of confocal z-stack images were taken with and without the field were acquired using a 60× water objective on a Ti-U inverted microscope (Nikon), a Carv II spinning disc confocal attachment (Becton Dickenson), and CoolSnap HQ CCD camera (Photometrics). Each stack was 10–15- μm thick with one z-stack every 0.4 μm to capture bead positions in the undeformed state as well as in the magnetic field-induced “rough” state. Traction force software based on three-dimensional image correlation was then able to track groups of particles to determine the displacements of the hydrogel in *x*-, y-, and *z*-dimensions, which were used to render a deformed surface [Fig. 1(A,B)]. Rendered surfaces had their roughness, R_{RMS} (root-mean-squared height),[26]

and spatial auto-correlation function computed as previously described.[27] Specifically, the one-half-height correlation length, that is, the peak-to-valley distance, was computed to estimate the size of the roughness features.

Material characterization-stiffness

Force-mode atomic force microscopy (AFM) was used to assess changes in bulk topography and Young's modulus, *E* (also called "stiffness") as previously described.[28,29] Hydrogel samples were placed on an MFP-3D-BIO atomic force microscope (Asylum Research; Santa Barbara, CA). Using custom Igor Pro software (Wavemetrics; Portland, OR), samples were indented in a regular array of points with a resolution of 0.1 points per μm^2 using a SiN cantilever with a spring constant k_{sp} = 20 pN/nm, a scan area of 3600 μm^2 as indicated, and an indentation velocity of 2 μm/s (40 nN/s loading rate). With the resulting deflection, cantilever spring constant, and assuming Hookean behavior for the cantilever, force *versus* hydrogel indentation spectrographs could be constructed.[30] From the change in deflection relative to the *z*-distance that the cantilever moved, topography of the sample can be calculated and modulus determined from a fit of the Hertz equation[31] using a linearized method.[32] With this fitting method, bilayered materials can be detected, and for indentations as deep as 2 μm, only a single modulus is observed [Fig. S1(A) in Supporting Information].

Cell culture and transfection

A7R5 rat smooth muscle cell line (ATCC) was cultured in Low Glucose Dulbecco's modified Eagle medium (DMEM; Gibco #18855) with 10% FBS, 2 m*M* glutamine, and antibiotics/antimycotics. Cells were passaged every 3 days as necessary. The plasmid, pTagRFP-N vector (courtesy of Dr. Shu Chien), was transformed into DH5α *E. coli* by heat shock at 42°C and selected and amplified LB broth with kanamycin. The plasmid was purified using the UltraClean 6-min Mini Plasmid Preparation Kit (Mo Bio Laboratories, #12300-100). One day before the transfection, 40,000–50,000 cells were plated in each well of a six-well plate and allowed to adhere and spread. On the day of the transfection, culture medium was removed and replaced with DMEM + 2% FBS (no antibiotics) to serum-starve cells. For each well, 4 μg of RFP-Actin were added to 250 μL of Opti-MEM Reduced serum medium. In a separate tube, 5 μL of Lipofectamine 2000 were added to 250 μL of Opti-MEM and incubated for 5 min at room temperature. The RFP-Actin and Lipofectamine were then gently mixed and incubated for 20 min at room temperature. The low-serum medium was then aspirated out of the wells, 1.5 mL of fresh low-serum medium (DMEM + 2% FBS, no antibiotics) and 500 μL of complexes were added to each well for 24 h. 24 h post-transfection, media was replaced with normal culture media. 72 h post-transfection, selection medium (Low Glucose DMEM with 10% FBS, and streptomycin, penicillin, and neomycin) was added to select for plasmid-expressing cells.72–96 h post-transfection, the cells expressed the highest levels of RFP-Actin and were replated onto hydrogels for experiments.

Cell-material interaction experiments

Changes in A7r5 cell area and morphology, as measured in real time using a 60× water objective on a Ti-U inverted microscope (Nikon) with a CoolSnap HQ CCD camera

(Photometrics), were observed under static and dynamic magnetic fields. For static topographical changes, cells were plated for several hours on the hydrogel to permit spreading. RFP-labeled cells were then observed immediately prior to addition of the field to establish steady state cell area and then continuously imaged for at least 1 h using a temperature controlled stage (ASI Imaging). All cell intensities for static experiments with time-lapse imaging were compensated for photobleach using control cells where no topography changes occurred. To achieve continual magnetic oscillation for dynamic topography, hydrogels were placed in an incubator-safe magnetic actuator where a motor moved the magnets into place below the hydrogel as with the static case and then far away from the hydrogel such that the magnetic field was essentially zero. Cycle frequency was maintained at 1 Hz. Cells were seeded onto microwire-embedded hydrogels and control hydrogel without microwires, allowed to adhere and spread for 4 h, and rinsed with media to remove all non-adherent cells prior to actuation. Cells were incubated under these conditions for the indicated amount of time, fixed, labeled, and mounted a slide for immunofluorescent imaging. Consistent with previous results,[3] most cells were not well-spread enough to observe well-defined, individual actin filaments but had well-defined spread areas as a result of transfection. Time-lapse movies from static cultures and preactuation and postactuation images from dynamic cultures were analyzed by Image J software (NIH) for area and morphology changes in cells exhibiting high RFP signal. Cell area, spindle factor (major divided by minor cell axis), and orientation correlation factor (OCF) were measured. OCF quantifies the alignment between two objects, in this case the cells and microwires, using equation 1:

$$\mathrm{OCF}=\frac{1}{2}[\cos(2\theta)+1] \quad (1)$$

which yields OCF = 1 (0) when the two objects are parallel (perpendicular). For the static experiment, cells with varying surface roughness between 0.175 μm and 0.522 μm (n = 12) as well as three control cells with no wires were analyzed. The data was binned by initial cell spread area into a control group, a “small” cell group (A_0 < 550 μm^2), and a “large” cell group (A_0 > 700 μm^2). The data was also binned by surface roughness into a control group, a “low” surface roughness group (R_{RMS} < 0.2 μm), and a “high” surface roughness group (R_{RMS} > 0.2 μm).

Statistics

All bar graph data is shown as the average ± standard deviation unless otherwise noted. Analysis of covariance (ANCOVA) was performed to assess significant between grouped data and student’s t-tests were used for simple paired comparisons. Significance was assessed for p values less than 0.05. All data was repeated in triplicate with the number of replicates indicated when counting individual cells.

RESULTS

Synthesizing and characterizing dynamic topography

A PA hydrogel using a two-step polymerization process was adopted to confine magnetic microwires, ~5 μm in diameter and 20 μm in length, to the surface of the hydrogel so that

they would provide a maximal torque on the surface. Polymer solutions were also kept dilute so that the ensuing hydrogel would be soft enough to ensure maximum deformation within a given magnetic field. Three-dimensional traction force microscopy software was used to track *x*-, *y*-, and *z*-bead displacements caused by surface deformations induced by magnetic actuation of the microwires. Displacements were then rendered into a 3D image of the deformed hydrogel surface [Fig. 1(A,B)]. Samples with varying wire concentrations were analyzed, and a strong positive correlation was found between wire density (as measured by the ratio of wire area to total view area) and surface roughness [Fig. 1(C)]; changes in surface roughness, ΔR_{RMS}, upon magnetic actuation ranged from 0.05 to 0.70 μm from an average starting roughness of less than 0.1 μm. Although R_{RMS} is a widely accepted metric, it is not able to fully characterize the spatial distribution of roughness on the surface, since it is highly dependent on feature amplitude. Therefore, an analysis of the spatial auto-correlation function of each surface was performed [Fig. 1(D) inset]. The size of the primary correlation lobe, which estimates the peak-to-valley distance between topographical features, ranged between 6 and 15 or 16 and 35 μm, depending on the feature axis is examined, i.e. minor or major respectively. Surprisingly, feature spacing was largely independent of roughness [Fig. 1(D)], indicating that even with multiple microwires present, feature width was uniform despite differences in roughness height. To confirm that these features were also not the result of thickness changes within the wire-containing second layer, bead images were also reconstructed as confocal cross-sections and indicated that there was no significant change in layer thickness across the hydrogel or as a result of magnetic actuation [Supporting Information Fig. S1(B)].

Two-layer PA hydrogels embedded with magnetic micro-wires deviate from previously characterized PA hydrogels,[21] so passive surface mechanics were measured prior to cell attachment. Undeformed topography and hydrogel stiffness were mapped by AFM [Fig. 2(A)]. Topography maps showed a relatively flat surface with a gradual slope of less than 80-nm height change per lateral micron [Fig. 2(B)], which is well below the minimum R_{RMS} and not likely an influence on cell behavior. Hydrogel stiffness when pressing directly above a microwire was slightly softer than regions lacking microwires [Fig. 2(C)]. Two-layer polymerization resulted in hydrogels several fold stiffer than a single layer PA hydrogel, so the absence of stiffening above a wire perhaps indicates that it prevented the second layer from mixing with the first and further polymerizing the hydrogel. Moreover, it is also possible to estimate an upper limit for the resulting wrinkle size from the brightfield and AFM map of the wire's size, which was less than 100 v μm^2, assuming that the wire deformed the entire surface are it occupies.

In addition to passive characterization, active hydrogel properties were measured. PA hydrogels have Poisson's ratios estimated to be 0.3–0.45,[3,33] so topographical and lateral displacements were compared to determine if and where *z*-displacements exceeded *x*- and *y*-displacements. The primary displacement plane varied depending on microwire orientation, so the comparison was performed for each hydrogel surface regardless of microwire density [Supporting Information Fig. S2(A,B)]. Although there was considerable spatial variability, global displacement ratios, where a value greater than 1 would imply a greater *z*-deformation, showed that *z*-displacements exceeded both *x*- and *y*-displacements

[Supporting Information Fig. S2(C)]. Second, deformation caused by the magnetic field rotating the microwires, either long-term static or dynamic, could potentially cause the hydrogel to undergo viscoelastic creep. Under constant magnetic field, no significant difference in the displacement field was observed between 0 [Supporting Information Fig. S3(A)] and 24 h [Supporting Information Fig. S3(B)] as compared to the undeformed state. Also, there was no significant change in displacement between the initial and final undeformed states, that is, no magnetic field at 0 and 24 h, indicating that plastic deformation did not occur. Thus, roughness appears to be independent of the amount of time the field is applied to the hydrogel [Supporting Information Fig. S3(C)]. No change in control samples also indicated that there was minimal microscope drift. Thus, altered cell behavior on this material in the presence of a magnetic field is likely dominated by topography changes so long as stiffness changes can be ruled out via control hydrogels lacking microwires.

Hydrogels also must be functionalized to permit cell attachment, but given the deformation magnitude required to change substrate roughness, it is also important to verify that the protein coating permitting cell adhesion does not change when the substrate is deformed. Confocal cross-sections through the hydrogel showed that regardless of the presence of the magnetic field, there was no appreciable change in the fluorescent intensity of fluorescently labeled fibronectin for wire-embedded hydrogels [Supporting Information Fig. S(4)]. Given the short duration of subsequent cell adhesion studies, it is not likely that this protein coating is sufficiently remodeled or that new matrix is deposited on top of it[34] to alter adhesion independent of topography.

Dynamic topography alters short-term but not long-term cell morphology

As cells remodel their environment, they may create either step changes in topography by isometrically contracting their matrix or dynamic changes by cyclically contracting their matrix. To assess the extent to which cells can respond to these changes in a soft matrix, VSMCs were allowed to attach to undeformed hydrogels. Cells were transfected with fluorescent actin for real time visualization as well as to encourage their spreading on such a soft substrate[3]; other cell types, e.g. mesenchymal stem cells, fail to have a robust spread morphology on substrates < 2 kPa.[18] Cells were first subjected to a static step change in topography. As shown in Figure 3, significant lamellipodial area and shape changes can be observed when the field is first turned on versus control cells. Cell area was normalized to the initial time point, grouped by cell size or surface roughness, and averaged. When binned by initial cell area, large cells ($A_0 > 700\ \mu m^2$) had statistically significant remodeling that occurred faster and to a greater extent than nonactuated cells of all sizes grouped together [Fig. 4(A)]. It is important to note that given the average VSMC size ($566 \pm 191\ \mu m^2$), surface roughness, our estimate of wrinkle size ($<100\ \mu m^2$), and feature spacing, even a small cell should interact with one or more wrinkles that are subcellular in size.

When binned by surface roughness, i.e. greater or less than 200 nm, all step topographical changes, regardless of roughness, had different responses *versus* control cells that were statistically significant. Interestingly, a step change in cell area was observed for cells on substrates with higher roughness [Fig. 4(B), green arrow], indicating a robust and immediate

response to a step change in substrate topography *versus* the more gradual change with less rough substrates. The gradual changes observed with area could be the result of a passive response to the presence of the wires at the surface but not the field itself as has been previously shown,[35] so to determine if the presence of microwires modified cell behavior, cell area and spindle factor, that is, a cells major/minor axis ratio, was measured in hydrogels with and without microwires. A ~30% change was observed between cells on substrates with and without microwires for both metrics after 1 h [Fig. 4(C), left]. This area change is similar to the total change observed with the magnetic field on, so only the step change in cell area for the most rough substrates, that is, $R_{RMS} > 200$ nm, likely indicates an active response to a topographical change [Fig. 4(B), green arrow). VSMCs could also preferentially align with the microwires, potentially mitigating roughness changes. To ensure that measurements were not biased from alignment, an OCF [Eq. (1)] was computed between microwires and cells; regardless of microwire actuation, alignment at 1 h was random since OCF was approximately 0.5 [Fig. 4(C), right].

Cell-matrix remodeling may also be less continuous and involve periodic contractions that displace or strain matrix fibrils via a cell's actin cytoskeleton.[36] As microwire-embedded hydrogels do not undergo viscoelastic creep or exhibit hysteresis [Supporting Information Fig. S2(C)], they can be cyclically actuated to mimic dynamic matrix topography without undergoing long-term, irreversible topography changes. After 1 h of cyclic actuation, surface roughness and cell area were loosely correlated (closed squares, $R^2 = 0.1$), especially compared to nonactuated substrates where no correlation was observed [Fig. 4(D)], but by 24 h in culture, cells did not show passive changes, align in the presence of wires, or exhibit a correlation between roughness and cell area (Fig. 5). Moreover, minimal VSMC proliferation was observed between 1 and 24 h (8077 ± 1994 and 8332 ± 197 cells/cm^2, respectively) and thus could not account for the lack of change. Thus, short-term responses to step changes in topography or cyclically actuated topography are detectable, but longer-term, cells remodel themselves to compensate for the topographical stimuli.

DISCUSSION

Soft hydrogels as a topographical substrate

The balance of the work performed to date to investigate topography's influence on cell function has involved rigid substrates where cell spreading among other responses is maximal.[5–7] These features, whether ordered or random,[9] play a dramatic role in regulating cytoskeletal rearrangements in stem cells to induce osteogenesis[8] or maintain potency.[26] Other cell types, for example, VSMCs, which require a softer niche also likely have some topographical preferences given that they inhabit a microenvironment consisting of fibrillar matrix,[2,11] but these rigid substrates would likely be less appropriate. To create dynamic topographical features within a softer substrate that avoids temperature[15,16] and reversibility issues,[14] we used a PA hydrogel system. These hydrogels can be orders of magnitude softer than the rigid substrates previously mentioned, and though they are also still largely elastic,[37,38] there may also be important viscous considerations.[39] Moreover, they have stiffness that is physiologically relevant for VSMCs.[3,12,40] These hydrogels needed to be compliant enough to permit sufficient microwire rotation so that roughness would change as

least 0.5 μm—a value likely to elicit a cell response—but not be so soft as to block cell spreading. A sequential polymerization process was also necessary to entrap beads and microwires at the surface but made predicting matrix elasticity difficult as previously observed in sequentially polymerized PA hydrogels.[41] Although softer hydrogels have roughness changes that could exceed this threshold, the PA hydrogels used here balanced both stiffness-induced spreading and topography dynamics. That said, PA hydrogels were still soft enough that few cells, including VSMCs which are generally large cells, could spread on matrix of similar stiffness and even then only when cytoskeletal components are overexpressed.[3] However when spread, cells were large enough so that the topographical features and softer microwire regions that they feel appear subcellular as with native matrix.[1,2]

Aside from compliance, soft substrates with dynamic topography have also shown significant feature anisotropy. Grooved substrates[10] and other regular patterns in soft surfaces[41] induce cell alignment which may be beneficial for ordered tissues, for example, muscle, but for those tissues with a less ordered matrix, randomly oriented features may be better. For example, semi-disordered topography on rigid substrates induced osteogenesis in stem cells.[9] Even other matrix cues such as ligand spacing benefit from semi-disordered presentation.[42] Here, microwires were randomly oriented from pipetting the wire-, bead-, and polymer-containing solution onto the PA surface to mimic topographical changes in fibrillar matrix[1,2] as best as possible with a hydrogel. However, aligned topography changes could also be produced by this system if necessary by applying the magnetic field prior to polymerization of the second layer. Rotation of the magnetic field would then produce regular, aligned deformations in the hydrogel that could mimic the more ordered soft substrates as shown elsewhere.[10,15,16]

Acute *versus* chronic responses to topography

The data here agrees with prior observations when force is applied acutely to a portion of the cell: immediately postapplication, cell focal adhesions grow at the site of force application,[24,43] but prolonged exposure results in a gradual decay in contractility.[24] Similarly, cutting a stress fiber results in an acute cell tension change, and the cell reorganizes its network to regain tensional homeostasis immediately.[44] Our VSMC data also appear consistent with actin cytoskeletal dynamics[45] where prolonged exposure to a stimuli could result in cytoskeletal rearrangements,[15] which would cause the lamellipodia changes observed here. Thus, it would appear that the time dependence observed with both these and our observations may be due to the time scale it takes for cells to internally rearrange their cytoskeleton to best cope with the changing environment.

These data on soft substrates, especially the results observed at 24 h where no significant morphological change was observed from dynamic topography, stands in stark contrast to those of stem cells cultured on rigid substrates with defined topography. Regardless of substrate chemistry,[7–9] stem cells on rigid substrates become osteogenic over week(s) in culture. The substrates used here were soft enough to not likely support significant stem cell spreading,[18] making direct comparison to longer-term stem cell data on rigid substrates difficult and more likely a reflection on stiffness-induced spreading. However, this is not to

say that matrix stiffness supersedes topography, whether static or dynamic. Further analysis of stem cell phenotype is warranted in substrates that are not rigid but which still induce a spread stem cell morphology. Understanding the converse experiment will also help identify whether stiffness and topography regulate the switch between a contractile and synthetic VSMC phenotype.

CONCLUSIONS

Here, we have demonstrated that the incorporation of magnetically actuated wires into a PA hydrogel can produce a topographical change up to roughness of 0.7 μm to investigate the effects of dynamic substrate topography and stiffness on VSMC behavior. Results demonstrated that cells respond to acute changes in topography on soft hydrogels but that prolonged exposure to and dynamic oscillation of a substrate with disordered topographical features results in modest if any changes in cell shape and spreading. Together these data suggest that magnetically actuated hydrogels may be a unique way to impose reversible topographical and/or mechanical changes on cells cultured on soft substrates.

Supplementary Material

Refer to Web version on PubMed Central for supplementary material.

ACKNOWLEDGMENTS

The authors like to thank Drs. Shu Chien, Sungho Jin, and Alex Fuhrmann at UCSD for providing the RPF-actin plasmid, advice on microwire fabrication, and AFM software, respectively, and Drs. Nathan Sniadecki (University of Washington) and Brenton Hoffman (Duke University) general help and advice.

Contract grant sponsor: National Institutes of Health; contract grant number: DP02OD006460

Contract grant sponsor: San Diego Skeletal Muscle Research Center; contract grant number: P30AR061303

REFERENCES

1. Reilly GC, Engler AJ. Intrinsic extracellular matrix properties regulate stem cell differentiation. J Biomech. 2010; 43:55–62. [PubMed: 19800626]
2. Hay, ED. Cell Biology of Extracellular Matrix. New York: Plenum Press; 1991.
3. Engler A, Bacakova L, Newman C, Hategan A, Griffin M, Discher D. Substrate compliance versus ligand density in cell on gel responses. Biophys J. 2004; 86:617–628. [PubMed: 14695306]
4. Isenberg BC, Dimilla PA, Walker M, Kim S, Wong JY. Vascular smooth muscle cell durotaxis depends on substrate stiffness gradient strength. Biophys J. 2009; 97:1313–1322. [PubMed: 19720019]
5. Curtis AS, Gadegaard N, Dalby MJ, Riehle MO, Wilkinson CD, Aitchison G. Cells react to nanoscale order and symmetry in their surroundings. IEEE Trans Nanobioscience. 2004; 3:61–65. [PubMed: 15382646]
6. Martinez E, Engel E, Planell JA, Samitier J. Effects of artificial micro- and nano-structured surfaces on cell behaviour. Ann Anat. 2009; 191:126–135. [PubMed: 18692370]
7. Oh S, Brammer KS, Li YS, Teng D, Engler AJ, Chien S, Jin S. Stem cell fate dictated solely by altered nanotube dimension. Proc Natl Acad Sci USA. 2009; 106:2130–2135. [PubMed: 19179282]
8. McNamara LE, McMurray RJ, Biggs MJ, Kantawong F, Oreffo RO, Dalby MJ. Nanotopographical control of stem cell differentiation. J Tissue Eng. 2010; 2010:120623. [PubMed: 21350640]

9. Dalby MJ, Gadegaard N, Tare R, Andar A, Riehle MO, Herzyk P, Wilkinson CD, Oreffo RO. The control of human mesenchymal cell differentiation using nanoscale symmetry and disorder. Nat Mater. 2007; 6:997–1003. [PubMed: 17891143]
10. Lam MT, Clem WC, Takayama S. Reversible on-demand cell alignment using reconfigurable microtopography. Biomaterials. 2008; 29:1705–1712. [PubMed: 18192004]
11. Discher DE, Janmey P, Wang YL. Tissue cells feel and respond to the stiffness of their substrate. Science. 2005; 310:1139–1143. [PubMed: 16293750]
12. Engler AJ, Richert L, Wong JY, Picart C, Discher DE. Surface probe measurements of the elasticity of sectioned tissue, thin gels and polyelectrolyte multilayer films: Correlations between substrate stiffness and cell adhesion. Surf Sci. 2004; 570:142–154.
13. Nivison-Smith L, Weiss AS. Alignment of human vascular smooth muscle cells on parallel electrospun synthetic elastin fibers. J Biomed Mater Res A. 2012; 100:155–161. [PubMed: 21997972]
14. Wang LF, Pai CL, Boyce MC, Rutledge GC. Wrinkled surface topographies of electrospun polymer fibers. Appl Phys Lett. 2009; 94:151916.
15. Davis KA, Burke KA, Mather PT, Henderson JH. Dynamic cell behavior on shape memory polymer substrates. Biomaterials. 2011; 32:2285–2293. [PubMed: 21224032]
16. Le DM, Kulangara K, Adler AF, Leong KW, Ashby VS. Dynamic topographical control of mesenchymal stem cells by culture on responsive poly(epsilon-caprolactone) surfaces. Adv Mater. 2011; 23:3278–3283. [PubMed: 21626577]
17. Rao RN, Falls DG, Gerrity RG, Sethuraman SN, Thiruvaiyaru DS. Intimal thickness and layering, and smooth muscle cell phenotypes in aorta of youth. Pathobiology. 2000; 68:18–28. [PubMed: 10859527]
18. Engler AJ, Sen S, Sweeney HL, Discher DE. Matrix elasticity directs stem cell lineage specification. Cell. 2006; 126:677–689. [PubMed: 16923388]
19. Rowlands AS, George PA, Cooper JJ-White. Directing osteogenic and myogenic differentiation of MSCs: Interplay of stiffness and adhesive ligand presentation. Am J Physiol Cell Physiol. 2008; 295:C1037–C1044. [PubMed: 18753317]
20. Tse JR, Engler AJ. Stiffness gradients mimicking in vivo tissue variation regulate mesenchymal stem cell fate. PLoS One. 2011; 6:e15978. [PubMed: 21246050]
21. Tse JR, Engler AJ. Preparation of hydrogel substrates with tunable mechanical properties. Curr Prot Cell Biol. 2010; 10:1–16.
22. Rajagopalan P, Marganski WA, Brown XQ, Wong JY. Direct comparison of the spread area, contractility, and migration of balb/c 3T3 fibroblasts adhered to fibronectin- and RGD-modified substrata. Biophys J. 2004; 87:2818–2827. [PubMed: 15454473]
23. Aguirre KM, McCormick RJ, Schwarzbauer JE. Fibronectin self-association is mediated by complementary sites within the amino-terminal one-third of the molecule. J Biol Chem. 1994; 269:27863–27868. [PubMed: 7961716]
24. Sniadecki NJ, Anguelouch A, Yang MT, Lamb CM, Liu Z, Kirschner SB, Liu Y, Reich DH, Chen CS. Magnetic microposts as an approach to apply forces to living cells. Proc Natl Acad Sci USA. 2007; 104:14553–14558. [PubMed: 17804810]
25. Del Alamo JC, Meili RB, Alonso-Latorre J, Rodriguez-Rodriguez Aliseda A, Firtel RA, Lasheras JC. Spatio-temporal analysis of eukaryotic cell motility by improved force cytometry. Proc Natl Acad Sci USA. 2007; 104:13343–13348. [PubMed: 17684097]
26. McMurray RJ, Gadegaard N, Tsimbouri PM, Burgess KV, McNamara LE, Tare R, Murawski K, Kingham E, Oreffo RO, Dalby MJ. Nanoscale surfaces for the long-term maintenance of mesenchymal stem cell phenotype and multipotency. Nat Mater. 2011; 10:637–644. [PubMed: 21765399]
27. Thomas TT. Recent advances in the measurement and analysis of surface microgeometry. Wear. 1975; 33:205–233.
28. Chirasatitsin S, Engler AJ. Detecting cell-adhesive sites in extracellular matrix using force spectroscopy mapping. J Phys Condens Matter. 2010; 22:194102. [PubMed: 21152375]

29. Flores-Merino MV, Chirasatitsin S, Lopresti C, Reilly GC, Battaglia G, Engler AJ. Nanoscopic mechanical anisotropy in hydrogel surfaces. Soft Matter. 2010; 6:4466–4470. [PubMed: 20953281]
30. Engler AJ, Rehfeldt F, Sen S, Discher DE. Microtissue elasticity: Measurements by atomic force microscopy and its influence on cell differentiation. Methods Cell Biol. 2007; 83:521–545. [PubMed: 17613323]
31. Radmacher M, Tillamnn RW, Fritz M, Gaub HE. From molecules to cells: Imaging soft samples with the atomic force microscope. Science. 1992; 257:1900–1905. [PubMed: 1411505]
32. Kaushik G, Fuhrmann A, Cammarato A, Engler AJ. In situ mechanical analysis of myofibrillar perturbation and aging on soft, bilayered Drosophila myocardium. Biophys J. 2011; 101:2629–2637. [PubMed: 22261050]
33. Boudou T, Ohayon J, Picart C, Tracqui P. An extended relationship for the characterization of Young's modulus and Poisson's ratio of tunable polyacrylamide gels. Biorheology. 2006; 43:721–728. [PubMed: 17148855]
34. Mao Y, Schwarzbauer JE. Stimulatory effects of a three-dimensional microenvironment on cell-mediated fibronectin fibrillogenesis. J Cell Sci. 2005; 118:4427–4436. [PubMed: 16159961]
35. Iwasaka M, Ueno S. Polarized light transmission of smooth muscle cells during magnetic field exposures. J Appl Phys. 2003; 93:6701–6703.
36. Giannone G, Dubin BJ-Thaler, Dobereiner HG, Kieffer N, Bresnick AR, Sheetz MP. Periodic lamellipodial contractions correlate with rearward actin waves. Cell. 2004; 116:431–443. [PubMed: 15016377]
37. Yeung T, Georges PC, Flanagan LA, Marg B, Ortiz M, Funaki M, Zahir N, Ming W, Weaver V, Janmey PA. Effects of substrate stiffness on cell morphology, cytoskeletal structure, and adhesion. Cell Motil Cytoskeleton. 2005; 60:24–34. [PubMed: 15573414]
38. Calvet D, Wong JY, Giasson S. Rheological monitoring of polyacrylamide gelation: Importance of cross-link density and temperature. Macromolecules. 2004; 37:7762–7771.
39. Cameron AR, Frith JE, Cooper JJ-White. The influence of substrate creep on mesenchymal stem cell behaviour and phenotype. Biomaterials. 2011; 32:5979–5993. [PubMed: 21621838]
40. Wong JY, Velasco A, Rajagopalan P, Pham Q. Directed movement of vascular smooth muscle cells on gradient-compliant hydrogels. Langmuir. 2003; 19:1908–1913.
41. Choi YS, Vincent LG, Lee AR, Kretchmer KC, Chirasatitsin S, Dobke MK, Engler AJ. The alignment and fusion assembly of adipose-derived stem cells on mechanically patterned matrices. Biomaterials. 2012; 33:6943–6951. [PubMed: 22800539]
42. Huang J, Grater SV, Corbellini F, Rinck S, Bock E, Kemkemer R, Kessler H, Ding J, Spatz JP. Impact of order and disorder in RGD nanopatterns on cell adhesion. Nano Lett. 2009; 9:1111–1116. [PubMed: 19206508]
43. Riveline D, Zamir E, Balaban NQ, Schwarz US, Ishizaki T, Narumiya S, Kam Z, Geiger B, Bershadsky AD. Focal contacts as mechanosensors: Externally applied local mechanical force induces growth of focal contacts by an mDia1-dependent and ROCK-independent mechanism. J Cell Biol. 2001; 153:1175–1186. [PubMed: 11402062]
44. Kumar S, Maxwell IZ, Heisterkamp A, Polte TR, Lele TP, Salanga M, Mazur E, Ingber DE. Viscoelastic retraction of single living stress fibers and its impact on cell shape, cytoskeletal organization, and extracellular matrix mechanics. Biophys J. 2006; 90:3762–3773. [PubMed: 16500961]
45. Ponti A, Matov A, Adams M, Gupton S, Waterman CM-Storer, Danuser G. Periodic patterns of actin turnover in lamellipodia and lamellae of migrating epithelial cells analyzed by quantitative Fluorescent Speckle Microscopy. Biophys J. 2005; 89:3456–3469. [PubMed: 16100274]

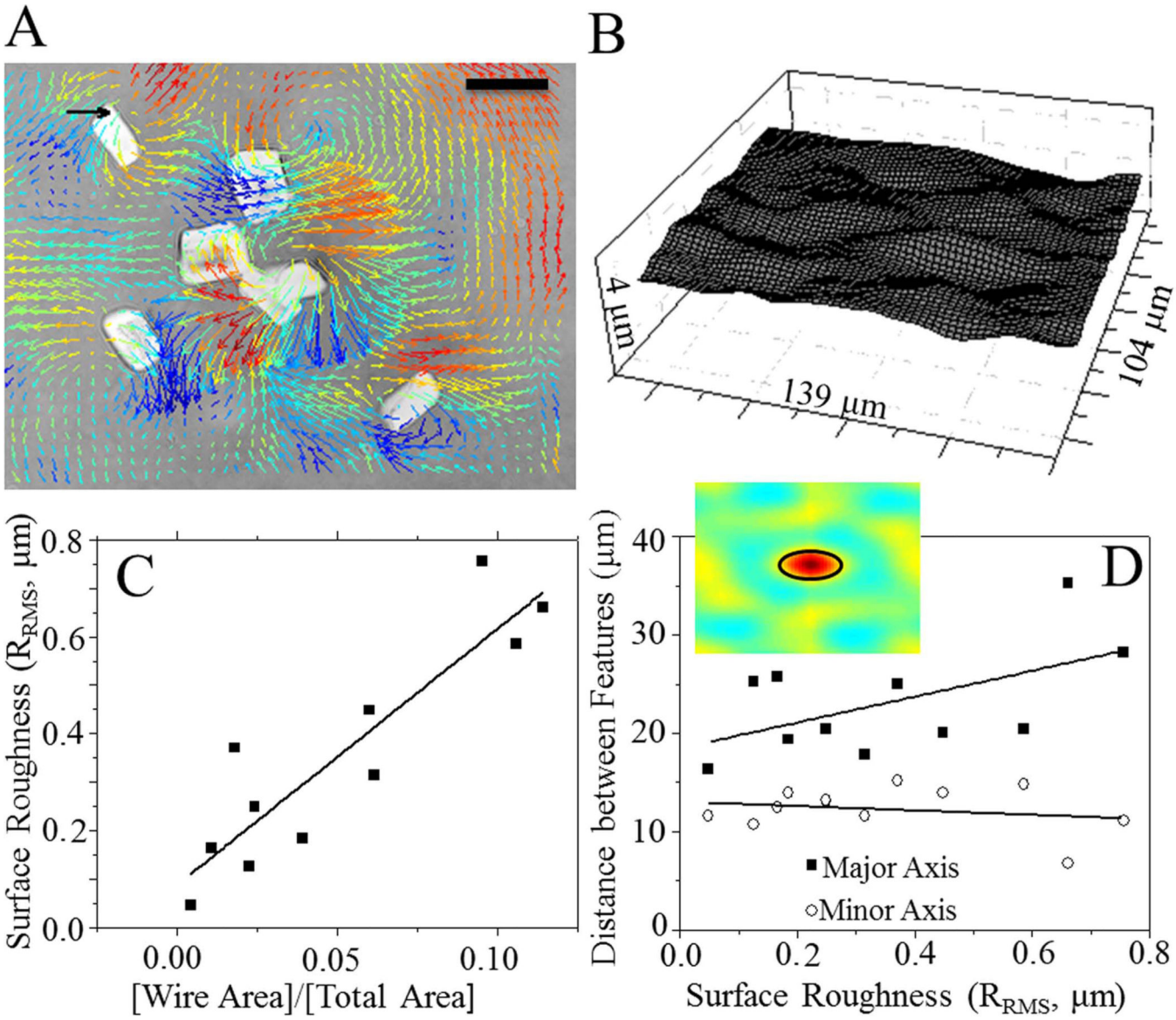

FIGURE 1.

Microwire-embedded matrix characterization. A: Displacement field induced by microwires in a 0.3 T magnetic field. Arrows indicate planar displacements whereas the color scale indicates *z*-displacements. Displacements were tracked by traction force microscopy (TFM) software. Warm (red) and cool (blue) colors correspond to positive and negative changes in *z*-relative to the undeformed surface. Scale bar = 20 μm. Black arrow = 5 μm displacement. B: Topographical map of surface feature changes. Features are on the order of 0.5–1.0 μm. C: A plot of the root-mean-square surface roughness (R_{RMS}) *versus* wire density (wire area divided by total surface area within an image) shows a positive correlation (R^2 = 0.81). D: Spatial correlation analysis showing the primary lobe that indicates the peak-to-valley distance between features (inset). The distance between features along the major and minor axis of each feature was plotted as a function of surface roughness with little change

observed as a function of surface roughness. [Color figure can be viewed in the online issue, which is available at wileyonlinelibrary.com.]

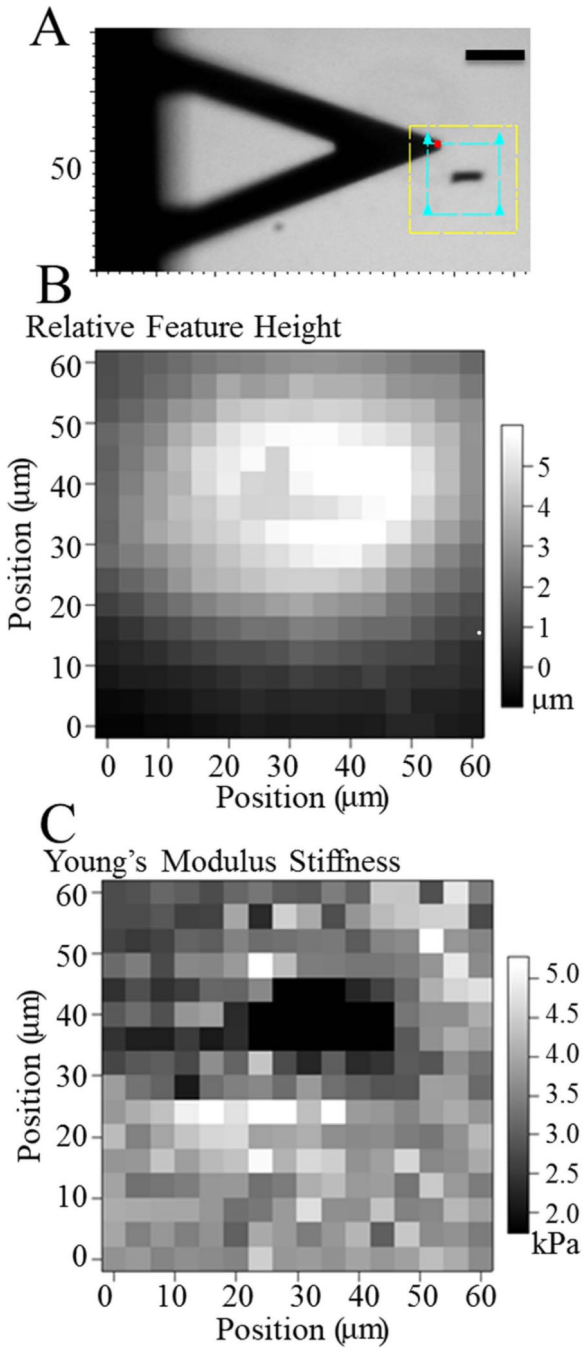

FIGURE 2.

Polymerization effects of microwires. A: Brightfield image of AFM scan area. Yellow box outlines the maximum scan area; blue box outlines the scan area used (60 × 60 μm^2). Scale bar = 50 μm. B: Relative surface topography of an undeformed PA hydrogel over the microwire shown in panel A. C: PA hydrogel stiffness shown for the microwire shown in panel A. [Color figure can be viewed in the online issue, which is available at wileyonlinelibrary.com.]

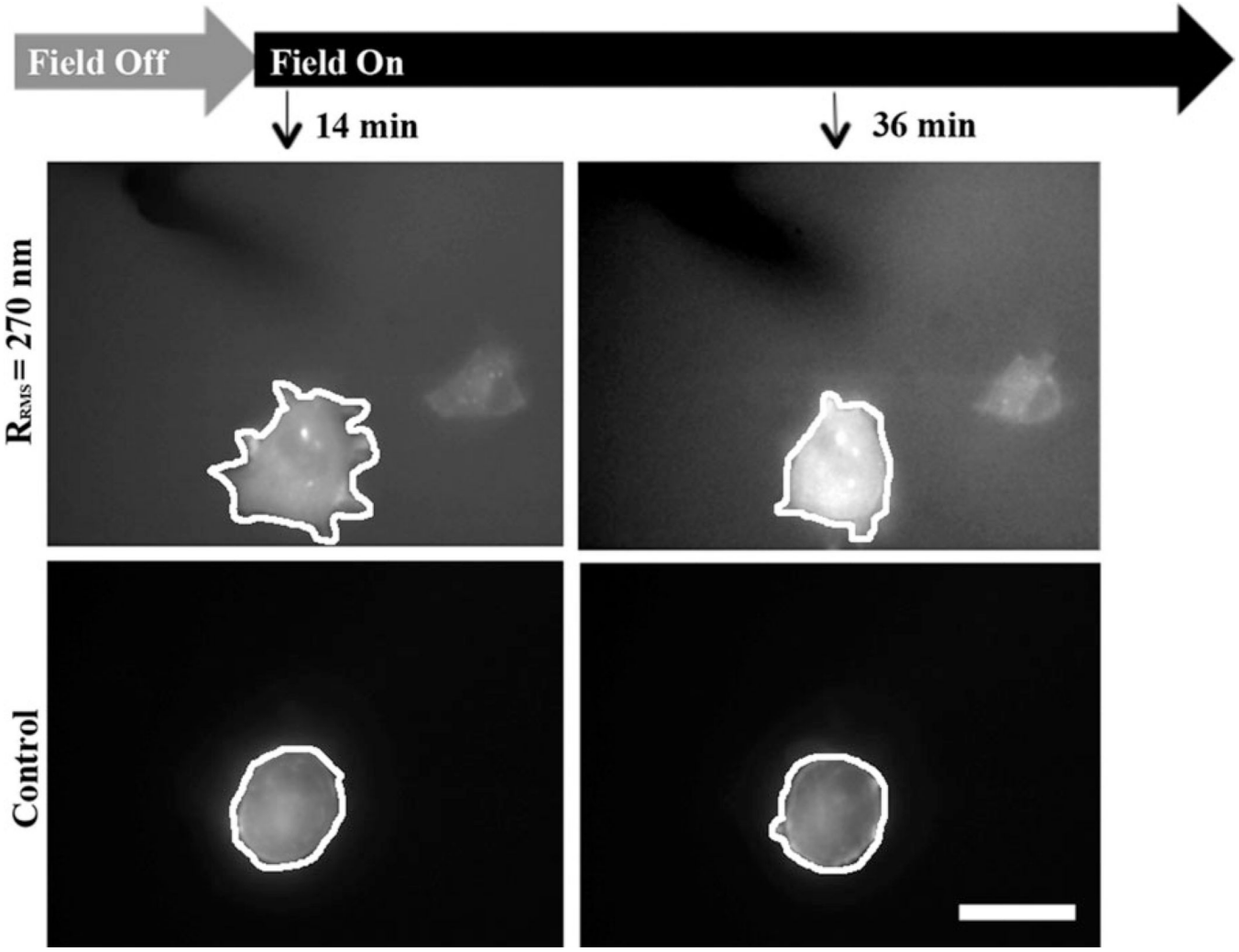

FIGURE 3.

Cells during a step topographical change. At the indicated times and magnetic field conditions (top), images were taken for an RFP-actin transfected cell on a hydrogel that was magnetically induced to have surface roughness of 270 nm (middle) and an RFP-actin transfected cell on a similar substrate without magnetic actuation (bottom). White lines have been added to illustrate the cell perimeter. Scale bar is 30 μm.

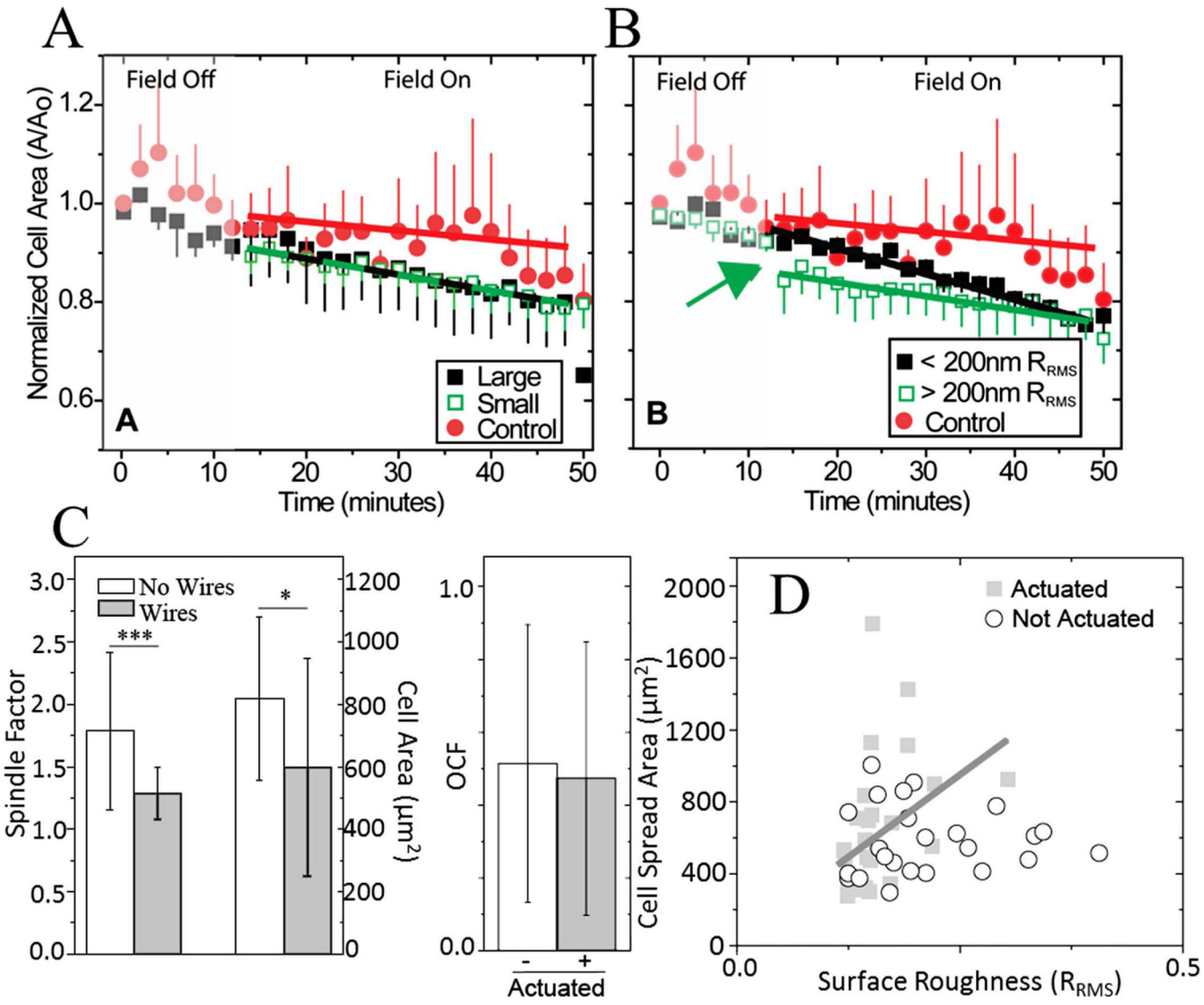

FIGURE 4.

Cell response to a step change and continuous modulation of topography after 1 h. Change in cell area (A/A_0) shown as a function of time when binned by (A) size and by (B) surface roughness for a step change in roughness when the field was turned on as indicated. ANCOVA between two groups indicated that in regard to cell size, only the difference between the control and large cells was statistically significant ($p < 0.001$) and for surface roughness, the difference between all of the groups was statistically significant ($p < 0.005$). Error bars are shown as standard error of the mean. C: On the left, cell spread area and shape factor shown as a function of the embedded microwires' presence after 1 h. ***$p < 0.001$, *$p < 0.05$. On the right, OCF was measured between cells and microwires for both the actuated and nonactuated substrates after 1 h of actuation ($p = 0.64$). D: Plot of the relationship between surface roughness and cell spread area for cyclically actuated and nonactuated substrates after 1 h of magnetic actuation. [Color figure can be viewed in the online issue, which is available at wileyonlinelibrary.com.]

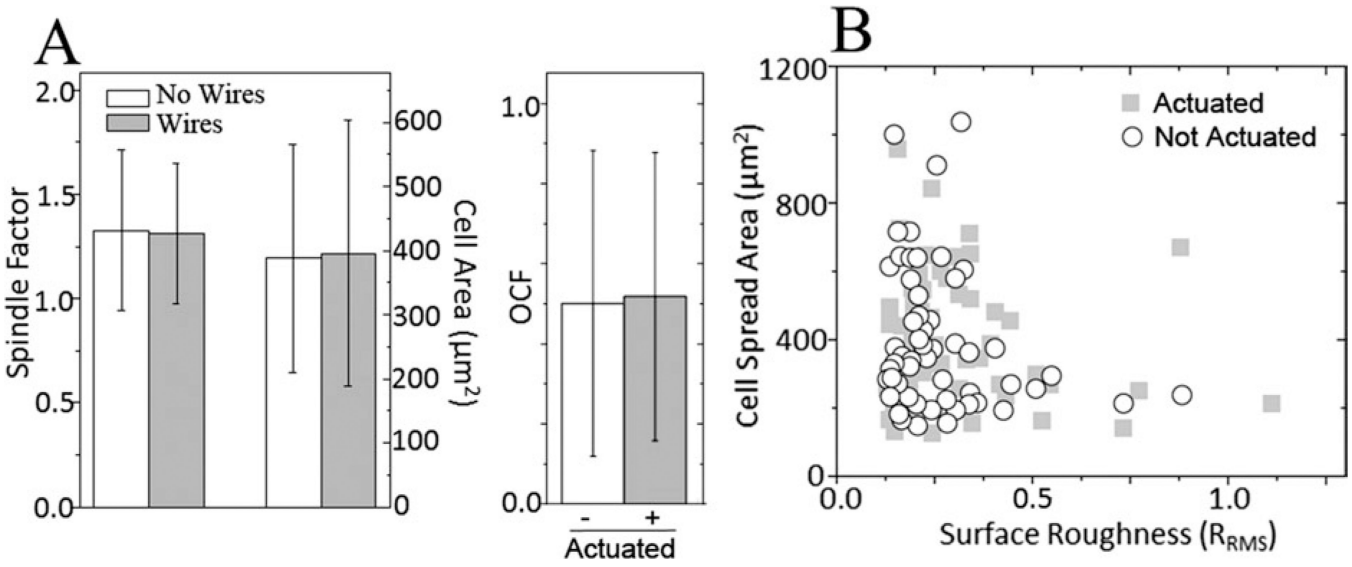

FIGURE 5.

Cell Response to Continuous Modulation of Topography at 24 h. A: On the left, the effect of the embedded microwires' presence on cell morphology without actuation was determined for cell spread area ($p = 0.93$) and shape factor ($p = 0.77$). On the right, OCF was measured between cells and microwires for both the actuated and nonactuated substrates ($p = 0.79$). B: Plot of surface roughness and cell spread area for actuated and nonactuated substrate.